HEFAT2014
10th International Conference on Heat Transfer, Fluid Mechanics and Thermodynamics
14 – 16 July 2014
Orlando, Florida

STARTING TRANSIENT SIMULATION OF A VACUUM EJECTOR-DIFFUSER SYSTEM UNDER CHEVRON EFFECTS

Fanshi Kong and Heuy Dong Kim*
*Author for correspondence
Department of Mechanical Engineering,
Andong National University,
Andong, 760-749,
South Korea,
E-mail: kimhd@anu.ac.kr

ABSTRACT

The vacuum ejector-diffuser system has been widely used in many applications such as refrigeration systems, high altitude test facilities and fluid transportation devices. In the present study, the starting transient flows of supersonic vacuum ejector-diffuser system, and its performance characteristics were simulated and analyzed by numerical methods. Newly designed chevron lobes were installed at the inlet of the primary stream of the vacuum ejector-diffuser system for the purpose of the performance improvement. A CFD method based on transient scheme has been applied to simulate the equilibrium flows and flow dynamics behavior of the secondary chamber. Primary numerical analysis results show that the chevrons get a positive effect on the vacuum ejector performance: less starting time and secondary chamber equilibrium pressure are found in chevron transient flow, compared with the convergent nozzle. The flow characteristics inside the ejector system are discussed using pressure history, vortices behavior, transient flow pattern and Reynolds stress distributions.

INTRODUCTION

As one of the important devices applied in the refrigeration systems [1,2], high altitude test facilities and fluid transportation industries [3], the vacuum ejector-diffuser system has been widely used due to its many incomparable advantages: such as no moving parts and even increasing pressure without mechanical energy [4-5]. The vacuum ejector-diffuser system is used to propel one low pressure secondary stream using high pressure primary stream through pure shear action. The mixing stream will flow out the ejector exit with a higher pressure than the secondary stream itself [6-7]. While in the vacuum ejector, the entrainment ratio between two streams is not so high like that of the normal ejector-diffuser system, and the secondary flow inlet of the vacuum ones is not supplied infinitely. This is due to its objective that not only to propel more secondary stream but also pull down the secondary chamber pressure as much as possible. In this case, the design of a vacuum ejector can not only base on the highest entrainment ratio (Rm), but also the volume of secondary chamber and pressure history during the operating process. In most of the earlier works [8-9], the secondary chamber was assumed to be of infinite size that can supply mass continuously. However in the most practical applications, the secondary chamber of the vacuum ejector has a finite volume. In this practical scenario, the starting transient flows of the vacuum ejector seems more meaningful than the final steady state itself [9-11].

In the present study, the steady cases with an infinite secondary stream was simulated to obtain the stable flow field. Then the secondary flow inlet was closed using wall boundary condition so that the left secondary mass can be pumped out due to the strong shearing action created by primary flow. Then the pressure inside the secondary chamber will be reduced. Present study is to simulate and analyse the starting transient flows of supersonic vacuum ejector-diffuser system, and its performance characteristics by numerical methods using a commercial software Fluent. Newly designed nozzle with several chevron lobes were installed at the inlet of the primary stream of the vacuum ejector-diffuser system for the purpose of its performance improvement. A CFD method based on transient scheme has been applied to simulate the equilibrium flows and flow dynamics behaviour of the secondary chamber. The flow characteristics inside the ejector system are discussed using pressure history, vortices behaviours, transient flow pattern and Reynolds stress distributions. RSM turbulent model was applied to simulate shear stress actions and vortices generation process, respectively, to demonstrate those effects on the starting transient process.

NOMENCLATURE

P	[Pa]	*Pressure*
Ps	[Pa]	Static pressure
P_0	[Pa]	Critical Pressure
$\dot{m}$	[kg/s]	Mass flow rate
max	[-]	Maximum
min	[-]	Minimum
R	[mm]	Radius of the nozzle
x	[mm]	Cartesian axis direction
y	[mm]	Cartesian axis direction
$y+$	[-]	Non-dimensional distance

NUMERICAL ANALYSIS

The setup of a vacuum ejector system was shown in the Figure 1, which represents the Setup of vacuum ejector using in the experiment [9]. As shown in this figure, the vacuum ejector constant of primary stream chamber, secondary stream chamber, mixing chamber and diffuser can be found obviously. The detailed geometrical parameters can be found in the reference [9], coupled with the results related to the present works.

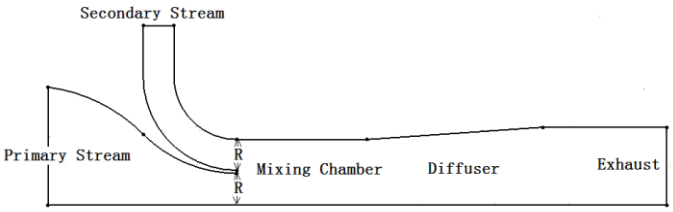

Figure 1 Setup of vacuum ejector used in the reference [9]

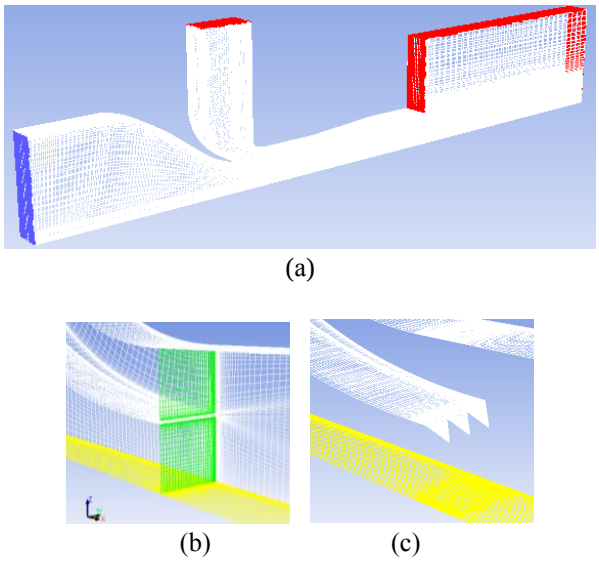

Figure 2 Comparative illustration of present CFD geometry with 3D display. (a) The vacuum ejector used in present CFD simulation; (b) Conventional convergent nozzle; (c) Newly designed optimal chevron nozzle.

In the present study, the computational model is based on 3-dimentional design due to the application of the chevron lobes, which have the shapes of triangular. The previous studies [6] showed the optimal geometries and lobe numbers of chevron nozzles. In this study, the chevron with optimal lobes were applied into the vacuum ejector system to study its performance improvement under chevrons effects.

At the same time, the CFD numerical geometrical model was built exactly same with the experimental data. Hence we can compare our results to the experiment ones. In the Figure 2, comparative illustration of present CFD geometry with 3D display is shown with a convergent nozzle. The red section represents the pressure outlet boundary condition, while the blue section is the pressure inlet boundary condition. As it is shown that, the exhaust exit of the ejector was extended using an box to stabilize the supersonic flow, and try to make the CFD results more accurate. The secondary stream inlet was taken as pressure inlet boundary at beginning and then the boundary condition was changed to wall to create a finite secondary flow.

Commercial software Gambit was used in the present research to create mesh domain. A structure mesh was employed in this case for ejector and quadrilateral cells were used in the mesh creation. The chevrons nozzle extent was made by unstructured mesh to achieve the lobes triangle shape. Boundary layer effects were considered by making finer grid densely clustered close to the walls. Systematic grid independence studies have been performed in this study for qualifying the grid size. Three separate grids were generated with 220000 cells, 430000 cells and 710000 cells. The first (coarse) grid has y+ of about 4.6. The second (medium) grid set has a y+ of about 2.7. The third (fine) set grid is generated using the same minimum space as the second set, but with much more cells. The computational domain with 430,000 cells was chosen because of its less computational time and more accurate result (Figure 2). The difference between CFD analysis and experimental results was less than 4%.

The axis symmetric, coupled implicit solver is chosen for the steady as well as unsteady simulations with boundary condition at inlet with the total pressure of 3 bars and total temperature of 300 K. At secondary inlet with pressure outlet boundary condition is given with total pressure as 1 bar and total temperature of 300 K. The boundary condition at exit is pressure outflow with back pressure of 1 bar; all the walls are adiabatic with no slip condition. Ideal gas was used as the working fluid in all cases. A finite volume scheme and density-based solver with coupled scheme were applied in the computational process. RSM turbulent model, implicit formulations were used considering the accuracy and stability. Second-order upwind scheme was used for turbulent kinetic energy as well as spatial discretizations. The flow is governed by the three-dimensional, compressible, steady-state/unsteady-state form of the fluid flow conservation equations. Reynolds Averaged compressible Navier–Stokes (RANS) equations are used in this work, which are more suitable for variable density flows.

RESULTS AND DISCUSSION

Figure 3 and Figure 4 show the contours of present CFD results compared between chevron nozzle and conventional nozzle, in terms of Mach number and density behaviour. Both the Mach number contours and density contours were similar from each other, while there is a small difference occurred near by the nozzle exit section. The chevron nozzle has vortexes while the convergent nozzle doesn't. Similar to those figures, Figure 5 is showing the contours comparison of static pressure between convergent nozzle and chevron nozzle, in a 3D display geometry. From the figure itself, is can be found that the high pressure primary stream flows out from the sonic nozzle and reduce rapidly due to a series of oblique shocks and expansion waves. Those waves create some Mach cones along the axis direction which are called diamond waves. Compare both nozzles' cases, the pressure distributions from the contours are similar to each other. The main difference is shown around the nozzle exit section and pressure inside the secondary chamber. The chevron nozzle with triangular lobes create some vortexes and make the flow unsteady until the vortexes become vortices system. Those eddies will develop into vortexes and finally create strong vortex shear actions. Under the chevrons influence, more longitudinal vortices were generated and the nozzle involve more secondary stream into the ejector. The mixing process was enhanced and more mass would be pumped out from the secondary chamber.

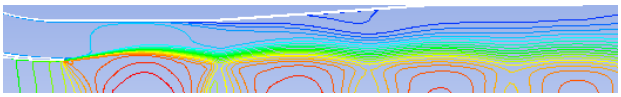

(a) Mach number contours of convergent nozzle

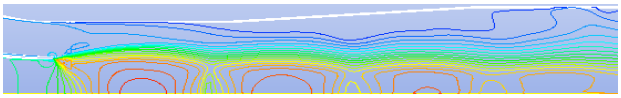

(b) Mach number contours of chevron nozzle

Figure 3 Mach contours of present CFD results

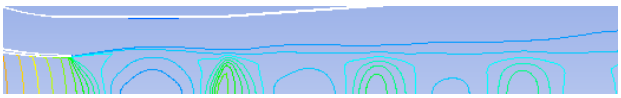

(a) Density contours of convergent nozzle

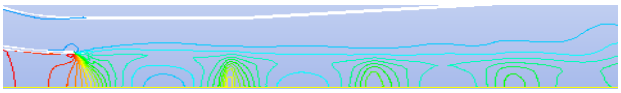

(b) Density contours of chevron nozzle

Figure 4 Density contours of present CFD results

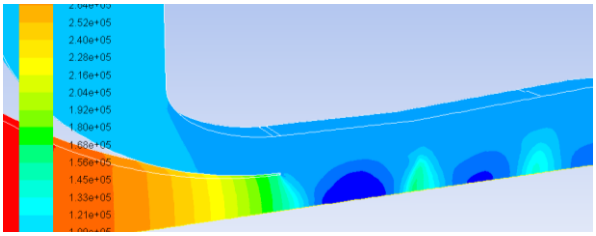

(a) Convergent nozzle

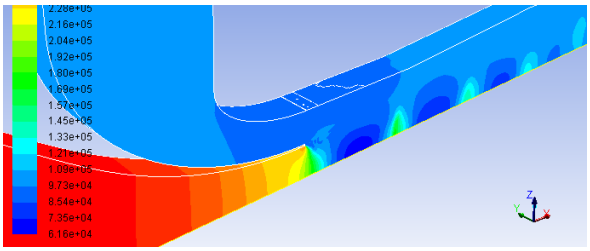

(b) chevron nozzle

Figure 5 Comparative contours of static pressure with 3D display geometry

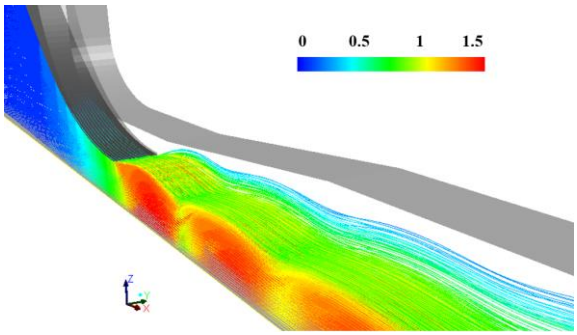

(a) Convergent nozzle

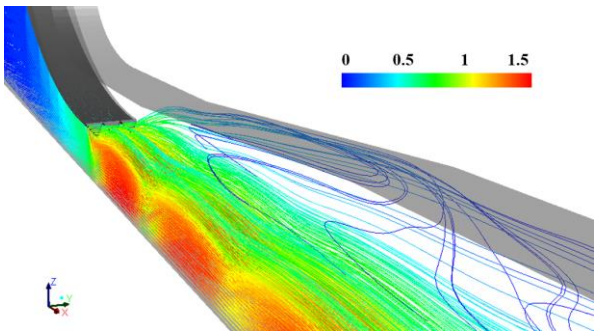

(b) chevron nozzle

Figure 6 Path lines distribution showing the longitudinal vortices of the chevron nozzle model

The generation process of the longitudinal vortex can be obviously found in the Figure 6. Of the particular is, longitudinal vortices were generated only by primary streams. That is why only the primary stream path lines were plotted. Compare two figures in the Figure 6, it can be obviously found that there are longitudinal flows generated under chevron effects, and only smooth path lines are formed in the convergent nozzle model. Initially, there is a small vortex generated between chevron lobes due to the unsteadiness. Then this vortex slowly develops along the flow direction and becomes bigger. The transversal vortex will transfer to longitudinal vortices when the vortex is close to the wall, and becomes strong in the following process. Strong longitudinal vortices bring in stronger shear stress between two streams and entrain more secondary flow into the chamber, which will lead the secondary chamber pressure much lower.

Figure 7 is showing the axial distributions of static pressure with both convergent nozzle and chevron nozzle. In this distribution, the chevron nozzle can be found higher pressure peak after the first shock wave. And a series of shock waves and expansion waves can be found after that. An interesting phenomenon is that the Mach number distribution become smoother after a series of strong shocks using the chevron nozzle. That also leads to more energy saving to propel more secondary stream into the vacuum ejector, which effectively enhanced its performance.

In the present paper, the time when the mass flow rate of secondary chamber equal to 0 is taken to define the state of equilibrium. As it is shown in the Figure 8, the mass flow rate history at the secondary chamber was shown, compared both convergent nozzle and chevron nozzle. At about 1.4 ms, the mass flow rate of secondary chamber in chevron nozzle case equal to 0, which means that the pressure inside the secondary chamber should also become the state of equilibrium. Compare to the convergent nozzle, the chevron nozzle used less time to approach the mass flow equilibrium state. Actually, after the flow get stable, the pressure will become fluctuate due to the unsteadiness of the flow. At the same time, the pressure inside the secondary will be strongly influence by the vortex generated near the nozzle exit.

Figure 9 shows the static pressure history at the secondary chamber. The experimental results based on steady solution has been plotted to compare with the CFD results. From the figure, it can be found that the chevron nozzle used less time to approach the pressure equilibrium state compare to the convergent one. From the analysis above, the results show that chevron nozzle leads to more energy saving, and more rotary flows would be entrained. Therefore, more shear stress will be generated to propel the secondary stream into the vacuum ejector, which will take less time to approach an equilibrium state. At the same time, it can be found that the equilibrium pressure after unsteady process seems to be lower in the chevron case. That is due to that more longitudinal vortices were generated and the nozzle involve more secondary stream into the ejector. The mixing process was enhanced and more energy transfer between two streams would happen. Therefore, the chevron nozzle has effectively generated more longitudinal vortexes and enhanced the performance of the vacuum ejector.

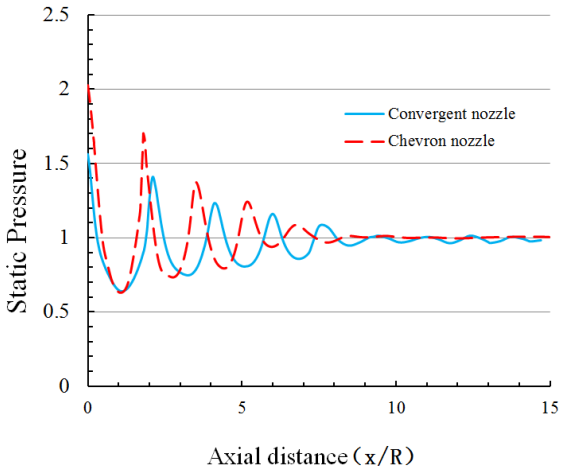

Figure 7 Axial distributions of static pressure with both convergent nozzle and chevron nozzle.

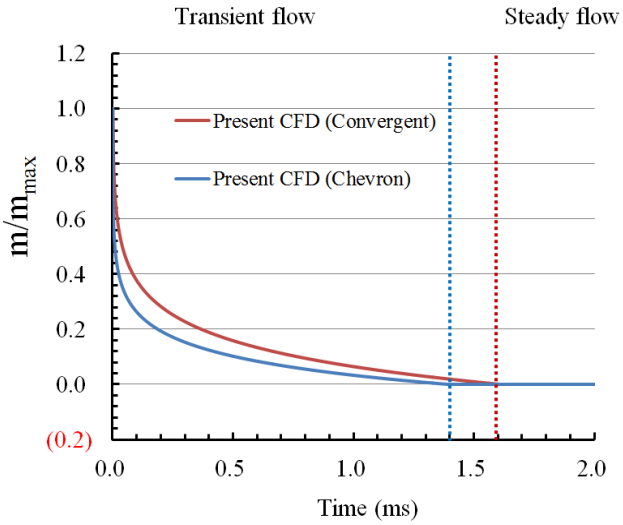

Figure 8 Mass flow rate history at the secondary chamber

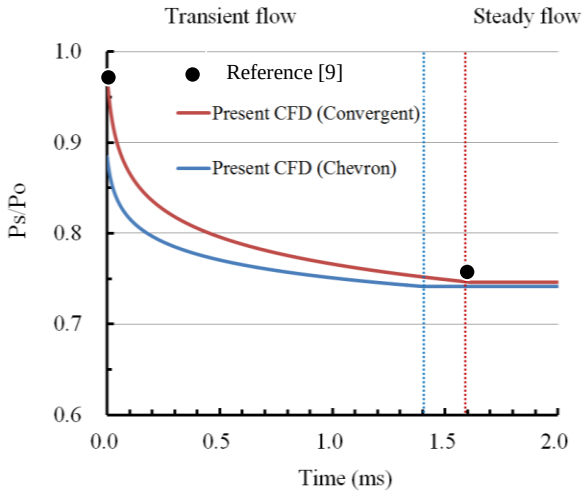

Figure 9 Static pressure history at the secondary chamber

CONCLUSION

In the present paper, a computational method was carried out to simulate the starting transient flow of a vacuum ejector system. The CFD results were validated by the pressure magnitude in the secondary chamber of the experimental results. The chevron nozzle effects on the performance of the ejector were investigated in detail. Numerical results were confirmed by previous experimental data. Based on the numerical analysis, less starting time (1.4 ms compare to 1.6 ms) and less secondary chamber equilibrium pressure (decreased about 3.2%) were found in chevron transient flow, compared with the conventional convergent one. Under the chevrons influence, more longitudinal vortices were generated, more rotary stream passed through the mixing chamber and introduced more shear stress to propel the secondary stream into the vacuum ejector. The mixing process was enhanced effectively and so did the performance of the vacuum ejector.

Further work is going on to study the physical behaviour of the vacuum ejector system with chevrons.

REFERENCES

[1] Sun, D., Variable geometry ejectors and their applications in ejector refrigeration systems. *Energy*, Vol.21, 1996, 919-929.

[2] Huang, B.J., Petrenko, V.A., Chang, J.M., Lin, C.P. and Hu, S.S., A combined cycle refrigeration system using ejector-cooling as the bottom cycle. *International Journal of Refrigeration*, Vol.24, 2001, pp.391-399.

[3] Blanco, J., Malato, S., Ferna ńdez-Iban˜ez, P., Alarco´n, D., Gernjak, W., and Maldonado M.I., Review of feasible solar energy applications to water processes. *Renewable and Sustainable Energy Reviews*, Vol.13, 2009, pp.1437-1445.

[4] Sankaran, S., Satyanarayana, T.V.V., Annamalai, K., Visvanathan, K., Babu, V. and Sundararajan, T., CFD analysis for simulated altitude testing of rocket motors. *Canadian Aeronautics and Space Journal*, Vol.48, 2002, pp.153-162.

[5] Desevaux, P. and Lanzetta, F., Computational fluid dynamic modeling of pseudoshock inside a zero-secondary flow ejector. *AIAA Journal*, Vol.42, 2004, pp.1480-1483.

[6] Kong, F.S., Kim, H.D., Jin, Y.Z. and Setoguchi, T., Computational analysis of mixing guide vane effects on performance of the supersonic ejector-diffuser system. *Open Journal of Fluid Dynamics*, Vol.2, 2012, pp.45-55.

[7] Östlund, J., Flow processes in rocket engine nozzles with focus on flow, separation and side-loads. Licentiate Thesis TRITA-MEK 2002:09, Department of Mechanics, Royal Institute of Technology, Stockholm, Sweden. 2002.

[8] Annamalai, K., Visvanathan, K., Sriramulu, V. and Bhaskaran, K.A., Evaluation of the performance of supersonic exhaust diffuser using scaled down models, *Experimental Thermal and Fluid Science*, Vol.17,1998, pp.217-229.

[9] Lijo, V., Kim, H.D., Rajesh, G., and Setoguchi, T., Numerical simulation of transient flows in a vacuum ejector-diffuser system, *Proceedings of the Institution of Mechanical Engineers, Part G: Journal of Aerospace Engineering*, Vol. 7, 2010, pp.777-786.

[10] Kim, H.D. and Lee, J.S., An experimental study of supersonic ejector for a vacuum pump. P*roceedings of the Korean Society of Mechanical Engineers, Annual Fall Meeting*. Vol.B, 1994, pp.520-525.

[11] Mittal, A., Rajesh, G., Kim, H.D., and Lijo, V., A Parametric Study on the Starting Transients of a Vacuum Ejector-Diffuser System, *Journal of Propulsion and Power*, in press, accepted manuscript (2013).